



Published in final edited form as:

Cancer. 2018 December 15; 124(24): 4657–4666. doi:10.1002/cncr.31761.

The anti-tumor effects of entinostat in ovarian cancer require adaptive immunity

DR. Haller J. Smith, MD¹, Tyler R. McCaw, BS², Angelina I. Londono, PhD³, Ashwini A. Katre, MSPH³, Selene Meza-Perez, PhD², Eddy S. Yang, PhD³, Andres Forero, MD⁴, Donald J. Buchsbaum, PhD³, Troy D. Randall, PhD², J. Michael Straughn Jr., MD¹, Lyse A. Norian, PhD⁵, and Rebecca C. Arend, MD¹

¹Division of Gynecologic Oncology University of Alabama at Birmingham, Birmingham, Alabama

²Division of Clinical Immunology and Rheumatology University of Alabama at Birmingham, Birmingham, Alabama

³Department of Radiation Oncology University of Alabama at Birmingham, Birmingham, Alabama

⁴Division of Hematology and Oncology University of Alabama at Birmingham, Birmingham, Alabama

⁵Department of Nutrition Sciences University of Alabama at Birmingham, Birmingham, Alabama

Abstract

Background: Ovarian cancer is poorly immunogenic; however, increased major histocompatibility complex class II (MHCII) expression correlates with improved immune response and prolonged survival in ovarian cancer patients. We previously demonstrated that the histone deacetylase inhibitor entinostat increases MHCII expression on ovarian cancer cells. This study evaluated whether entinostat treatment and resultant MHCII expression enhanced beneficial immune responses and impaired tumor growth in mice with ovarian cancer.

Methods: C57BL/6 mice bearing i.p. ID8 tumors were randomized to treatment with entinostat 20 mg/kg/day versus control. Changes in mRNA expression of 46 genes important for anti-tumor immunity were evaluated using NanoString[®], and multi-color flow cytometry was used to measure changes in protein expression and tumor-infiltrating immune cells.

Corresponding Author: Rebecca C. Arend, MD, 1700 6th Avenue South, Room 10250, Birmingham, Alabama 35249, rarend@uabmc.edu, 205-934-4986.

Author Contributions: Haller J. Smith – conceptualization, data curation, formal analysis, investigation, writing – original draft. Tyler R. McCaw – formal analysis, methodology, validation, writing – review and editing. Angelina I. Londono – formal analysis, investigation, methodology, supervision. Ashwini A. Katre – project administration, resources, supervision. Selene Meza-Perez – investigation, methodology, validation. Eddy S. Yang – conceptualization, methodology, resources, software, writing – review and editing. Andres Forero-Torres - conceptualization, methodology, resources, writing – review and editing. Donald J. Buchsbaum - conceptualization, methodology, resources, supervision, validation, visualization, writing – review and editing. Troy D. Randall - conceptualization, methodology, resources, supervision, validation, visualization, writing – review and editing. J. Michael Straughn, Jr. – resources, visualization, writing – review and editing. Lyse A. Norian - conceptualization, methodology, resources, supervision, validation, visualization, writing – review and editing. Rebecca C. Arend – conceptualization, formal analysis, funding acquisition, investigation, methodology, resources, supervision, validation, writing – review and editing.

Conflict of Interest: The authors have no relevant conflicts of interest to report.
The authors have no relevant conflicts of interest or pertinent financial disclosures to report.

Results: Entinostat treatment decreased growth of both s.c. and omental ID8 tumors and prolonged survival in immunocompetent C57BL/6 mice. NanoString® analysis showed significant changes in mRNA expression in 21 of 46 genes, including increased expression of the MHC I pathway, CIITA, interferon gamma, and granzyme B. C57BL/6 mice treated with entinostat had increased MHCII expression on omental tumor cells and higher frequency of tumor-infiltrating CD8+ T cells by flow cytometry. In immunocompromised mice, treatment with entinostat had no effect on tumor size and did not increase MHCII expression.

Conclusions: In this murine ovarian cancer model, entinostat treatment enhances beneficial immune responses. Moreover, these anti-tumor effects of entinostat are dependent on an intact immune system. Future studies combining entinostat with checkpoint inhibitors or other immunomodulatory agents may achieve more durable anti-tumor responses in ovarian cancer patients.

Precis:

The histone deacetylase inhibitor entinostat increases MHCII expression, enhances anti-tumor immune response, and impairs tumor growth in a murine ovarian cancer model.

Keywords

entinostat; ovarian cancer; MHCII; adaptive immunity

Introduction

Although approximately 75% of ovarian cancer patients will achieve clinical remission with a combination of surgery and taxane/platinum chemotherapy, the majority of patients will relapse and ultimately die of their disease [1]. The introduction of targeted therapies has done little to impact overall survival for women with ovarian cancer, and response to immunotherapy has been disappointing with overall response rates of ~15% with currently available checkpoint inhibitors [2–5].

Epigenetic changes, which alter gene expression without modifying the underlying DNA sequence, play an important role in cancer pathogenesis. One of the most common epigenetic pathways involves acetylation of lysine residues on the amino-terminal tails of histone proteins. Histone acetyl transferases (HATs) add negatively charged acetyl groups to neutralize histone charge and convert chromatin into a more transcriptionally permissive state, while histone deacetylases (HDACs) antagonize this process and lead to transcriptional repression and gene silencing [6]. 18 HDACs have been identified and divided into four classes based on sequence homology with yeast [7]. The class I HDACs are the most prevalent and are expressed at high levels in ovarian cancer, where their expression has been correlated with the development of platinum resistance and decreased survival in patients [8–10].

Several HDAC inhibitors have received FDA approval, all of which act by targeting the zinc ion required for catalytic action of the class I, II, and IV HDACs [11]. These agents can directly inhibit tumor growth via a variety of mechanisms, including cell cycle arrest, inhibition of angiogenesis, and promotion of apoptosis [7]. Additionally, HDAC inhibitors

can indirectly contribute to disease control by rendering tumor cells more immunogenic, and upregulating antigen presentation pathways and costimulatory surface molecules [12–15]. Our group and others previously demonstrated that entinostat, a class I specific benzamide HDAC inhibitor, leads to increased major histocompatibility complex II (MHCII) expression on ovarian cancer cells [16], a phenotype that correlates with higher numbers of tumor-infiltrating lymphocytes and improved survival [17–19].

In this study, we evaluated the effects of entinostat on the adaptive immune response in a syngeneic murine ovarian cancer model. We found that entinostat treatment of ovarian tumor-bearing mice led to a reduction in tumor growth and prolonged survival. In whole tumor lysates, genes involved in antigen presentation, T cell inhibition and exhaustion, and T cell effector function were differentially expressed following entinostat treatment. These observations correlated with an increase in tumor-infiltrating CD8⁺ T cells and were found to be contingent on adaptive immunity.

Methods

Cell lines and culture

The ID8 murine epithelial ovarian cancer cell line was provided by Dr. Yancey Gillespie (University of Alabama at Birmingham, Birmingham, Alabama). Cells were maintained in RPMI1640 (Mediatech, Inc.) supplemented with 10% fetal bovine serum (FBS, Atlanta Biologicals). Cells were passaged by dissociation with 0.05% trypsin, 0.53mM EDTA without sodium bicarbonate (Corning), washing, and reculturing. Cells were maintained in culture less than 10 passages from the parent stock. Experiments were performed at 70–80% confluency.

Mouse studies

All animal studies were approved by the University of Alabama at Birmingham Institutional Animal Care and Use Committee (IACUC). Immunocompetent C57BL/6 mice were obtained from Charles River Laboratories International. Rag1 knockout mice, which lack T and B lymphocytes, were obtained from The Jackson Laboratory. Experiments were performed in mice at 7–8 weeks of age.

For subcutaneous (s.c.) tumor models, mice were injected in the right flank with 7×10^6 ID8 cells in a 1:1 mixture of phosphate-buffered saline (PBS, Mediatech, Inc.) and growth-factor reduced Matrigel[®] Matrix basement membrane (Discovery Labware, Inc.). Mice were weighed weekly, and tumors were measured with calipers twice weekly in two dimensions (length x width). Treatment was started when the majority of mice in each group had tumors measuring at least 16 mm², which took approximately 30 days post ID8 cell injection. For intraperitoneal (i.p.) tumor models, mice were injected i.p. with 7×10^6 ID8 cells in 200 μ l PBS. Treatment was started 28 days after injection.

Mice were randomized to 14 days of treatment with either entinostat 20 mg/kg (LC Laboratories) dissolved in 70% PBS, 20% Kolliphor[®] EL (Sigma-Aldrich), and 10% dimethyl sulfoxide (DMSO, Sigma-Aldrich) or with vehicle control. Treatments were administered i.p. At the conclusion of the treatment period, mice were either euthanized or

observed for survival analysis. Omental tumors were harvested for flow cytometry and NanoString[®] analysis.

NanoString[®] nCounter mRNA analysis

C57BL/6 mice were injected with ID8 cells i.p. and treated with entinostat or vehicle control for 14 days as above. Omental tumors were subsequently harvested, and mRNA was extracted using the TRIzol[®] Plus RNA Purification Kit (Life Technologies Corporation). 500 μ L of TRIzol[®] Reagent was added to each tumor sample. Tumors were homogenized manually using a mortar and pestle and subsequently passaged 5–10 times through an 18-gauge syringe. The remainder of RNA extraction was performed according to manufacturer instructions. RNA quantification was performed using the DeNovix DS-11 Spectrophotometer (Denovix, Inc.). Samples were processed on the NanoString[®] nCounter Flex system per manufacturer instructions using a custom 46-gene immune panel designed based on the work of our group and others to interrogate genes involved in adaptive immunity (see Supplementary Table 1 for full list of genes). Expression levels were normalized to housekeeping genes. Analysis was performed using nSolver 2.6 software (NanoString Technologies). Cluster 3.0 and Java TreeView-1.1.6r4 were used to create heat maps.

Flow cytometry

Omental tumors were fragmented with scissors, and placed in 2 mL of Iscove's modification of DMEM (Corning) supplemented with 3.5% bovine serum albumin (Sigma), 0.5 mg/mL collagenase (Sigma), and 70 μ g/mL DNase I. Tumor fragments were placed in an orbital shaker at 250 rpm for 30 minutes at 37C and subsequently filtered through 70 μ m nylon strainers (Corning). The following antibodies were used for staining: PDL1 (12–5982-83), CD3 (47–0032-82), FoxP3 (25–5773-82), and CD45.2 (17–0454-82) (all from eBioscience), CD8 (560776) and CD25 (557192) (BD Biosciences), CD4 (560782, BD Horizon), IA/IE (107627, Biolegend), and LIVE/DEAD red fixable dye (Life Technologies). Fixation and permeabilization were performed using the FoxP3/Transcription Factor Staining Buffer Set (eBioscience). Samples were run using a BDFACS Canto II (BD Biosciences). Data were analyzed with FlowJo version 9.9.

Statistical analysis

All statistical analyses were performed using GraphPad Prism version 7.0. Tumor areas, mean normalized gene expression, mean fluorescent intensity (MFI), and percentages of infiltrating immune cells were compared using independent two-tailed t-tests with alpha of 0.05. Survival analysis was performed using the Kaplan Meier method, and curves were compared with the Mantel-Cox log-rank test.

Results

Entinostat inhibits tumor growth and prolongs survival in a murine ovarian cancer model

Several studies demonstrate diverse anti-cancer effects of HDAC inhibitors [7, 12–14], but their impact on ovarian cancer is less well defined. Here, we first evaluated the anti-tumor effects of entinostat in immunocompetent s.c. and i.p. murine ovarian cancer models. In the

s.c. model, entinostat led to a significant reduction in tumor growth compared to vehicle control by day 11 of treatment (19.9 ± 7.5 vs. 32.9 ± 9.7 mm², $p=0.046$), and this difference persisted at day 14 (19.0 ± 11.2 vs. 35.0 ± 5.8 mm², $p=0.022$) (Figure 1A). In the i.p. model, entinostat led to a significant decrease in omental tumor weight compared to vehicle control after 14 days of treatment (44.7 vs. 100.4 mg, $p<0.001$). At the time mice were sacrificed, only 1 of 5 mice treated with entinostat had visible ascites compared to 4 of 5 mice treated with vehicle control (Figure 1B). A separate cohort of C57BL/6 mice ($n=5$ per group) bearing i.p. tumors was similarly treated with entinostat or vehicle control for 14 days and overall survival (OS) measured (Figure 1C). Entinostat treatment led to a significant prolongation in median OS compared to vehicle control (74 vs. 62 days, $p=0.005$). The hazard ratio for death in the entinostat-treated mice was 0.26 (95% CI 0.06 to 1.21). These results indicate that daily entinostat treatment is able to significantly reduce ovarian tumor size and prolong survival in immunocompetent mice.

Entinostat induces changes in mRNA expression of genes important in anti-tumor immunity

HDAC inhibitors are estimated to alter the expression of approximately 22% of genes, thereby broadly affecting tumor and immune cell phenotypes, and collectively resulting in pleiotropic effects on the anti-tumor immune response [20]. In order to more comprehensively assess the effects of entinostat on the tumor-infiltrating immune response, we used the NanoString[®] assay to evaluate expression of 46 genes predominantly related to adaptive immunity in RNA extracted from omental tumors of C57BL/6 mice ($n=5$ per group) treated with entinostat or vehicle control. One mouse from each group had insufficient RNA quality for analysis, and as a result was excluded from final analysis, leaving 4 evaluable mice per group. Unsupervised hierarchical clustering showed distinct gene expression patterns in omental tumors of mice treated with entinostat compared to vehicle control (Figure 2A). When mean normalized expression values were compared, treatment with entinostat resulted in significant changes in mRNA expression in 21 of the 46 genes evaluated (Supplementary Table 1). Notably, we saw increases in expression of the effector T cell-related molecules, interferon gamma (IFN γ) (8.5 vs. 2.9, $p=0.04$), granzyme B (125.4 vs. 9.5, $p=0.01$), and CXCL10 (1,636.4 vs. 417.0, $p=0.02$) (Figure 2B). The immune checkpoint molecule PD-L1 was also upregulated (1,090.6 vs. 294.2, $p=0.02$) (Figure 2C), which is not unexpected, as it is positively regulated by IFN γ [21]. Expression of the immune checkpoint molecules LAG3 and BTLA were significantly decreased with entinostat treatment (Figure 2C), whereas expression of PD1 and CTLA4 were unchanged (Supplementary Table 1). Entinostat treatment also downregulated FoxP3 expression, suggesting decreased immune suppression by regulatory T cells. Treatment with entinostat also resulted in significantly increased expression of all of the MHC I alpha chains as well as CIITA (267.4 vs. 132.1, $p=0.01$); however, we did not observe a difference in expression of I-A or I-E alpha or beta chains at the mRNA level (Figure 2D, Supplementary Table 1). These changes in gene expression suggest that entinostat alters the tumor microenvironment by upregulating antigen presenting machinery as well as PD-L1, while also contributing to a more robust T cell response.

Entinostat increases MHCII protein expression on omental tumor cells

Recently, we demonstrated that entinostat increased MHCII expression on ovarian cancer cells *in vitro* and *in vivo*, using a spontaneously developing murine ovarian cancer model [16]. In order to extend those findings to our current model, we used flow cytometry to evaluate MHCII and PD-L1 expression in omental tumors of C57BL/6 mice treated with entinostat or vehicle control (n=5 per group). Expression of the common leukocyte antigen, CD45, was used to identify tumor-infiltrating immune cells, while those lacking CD45 expression were taken to be tumor or non-leukocytic stromal cells. This allowed comparison of protein expression levels using MFI. C57BL/6 mice treated with entinostat had significantly increased MHCII expression on tumor/stromal cells compared to those treated with vehicle control (1,585.0 vs. 581.4 MFI, p=0.002) (Figure 3A). There was a trend towards increased PD-L1 expression in the entinostat-treated mice; however, this was not statistically significant (2,832.0 vs. 1,593.0 MFI, p=0.05) (Figure 3B). Thus, our results indicate that entinostat is able to induce surface expression of MHCII molecules in the syngeneic, i.p. ID8 model of ovarian cancer.

Entinostat increases the frequency of CD8+ T cells in omental tumors

Having demonstrated increased expression of MHCII on the surface of tumor cells in multiple ovarian cancer models, as well as increased transcription of immune effector genes, we hypothesized that entinostat treatment would subsequently increase the frequencies of tumor-infiltrating lymphocytes. To test this, omental tumors were harvested from C57BL/6 mice that were treated with entinostat or vehicle control (n=5 per group). Tumor-infiltrating lymphocytes were identified using flow cytometry, gating first on live, CD45+ singlets, followed by CD8+, CD4+, or the regulatory T cell markers CD25+FoxP3+ (Figure 4A). Treatment with entinostat led to an increase in the frequency of CD8+ T cells present in the tumor (21.0% vs. 18.0%, p=0.04). There were no differences in the frequencies of CD4+ T cells (27.4% vs. 29.4%, p=0.25) or CD25+FoxP3+ regulatory T cells (4.7% vs. 3.4%, p=0.07) (Figure 4B). These data suggest that entinostat treatment leads to intratumoral accumulation of cytotoxic CD8+ T cells, while leaving CD4+ and regulatory T cell populations largely unaffected.

An intact immune system is required for the anti-tumor effects of entinostat

We next evaluated the relative contributions of direct cytotoxic and cytostatic effects versus immune-mediated effects on tumor growth as well as MHCII and PDL1 expression. Following the same protocol as used for the C57BL/6 mice, Rag1 knockout mice, which lack T and B cells, were challenged i.p. with ID8 tumors (n=6 per group), then treated with either entinostat or vehicle control for 14 days and subsequently euthanized. In these immunocompromised mice, there was a trending but non-significant reduction in omental tumor weight in mice treated with entinostat compared to vehicle controls (54.3 vs. 79.8 mg, p=0.09), and 4/6 mice in each group had visible ascites at the time of tumor harvest (Figure 5A). This slight difference likely reflects the direct cytotoxic and cytostatic effects of entinostat on tumor cells. By flow cytometry, there was no difference in MHCII (1,250.0 vs. 1,483.0 MFI, p=0.15) or PD-L1 surface expression (805.8 vs. 706.0 MFI, p=0.26) on tumor cells in Rag1 knockout mice treated with entinostat compared to control (Figure 5B). Again,

cells lacking CD45 expression were assumed to be tumor or non-leukocytic stromal cells. These data suggest that entinostat alone cannot induce MHCII expression on ID8 i.p. tumors, but instead, requires adaptive immunity to both induce MHC II expression on CD45- cells and control tumor outgrowth.

Discussion

In this study, we demonstrate that the anti-tumor activity of the class I-specific HDAC inhibitor entinostat in a murine model of ovarian cancer is dependent on the drug's ability to enhance the adaptive immune response. In C57BL/6 mice with an intact immune system, treatment with entinostat resulted in significantly decreased tumor size and less ascites formation; however, in Rag1 knockout mice, which lack functional lymphocytes, these effects were lost. This suggests that the efficacy of entinostat in our syngeneic model is not due entirely to direct cytotoxic or cytostatic effects of the drug, but rather occurs predominantly through an indirect mechanism that involves stimulation of adaptive immunity.

Entinostat treatment increased the percentages of CD8+ T cells present in tumors, and increased mRNA expression of IFN γ and granzyme B detected by NanoString[®] analysis. This finding suggests that intra-tumoral CD8+ T cells are activated and exerting cytotoxic effector functions within the tumor microenvironment. While the increase in mean normalized expression of IFN γ detected by NanoString[®] was relatively small, this may be due to the use of whole tumor lysate, wherein the T cell transcripts are diluted simply by mass effect. Moreover, substantial increases in the IFN γ -inducible genes CXCL10, MHCI, CIITA, and PDL1 supports the notion that the observed increase in IFN γ expression is sufficient to drive significant downstream effects in the presence of entinostat. In fact, it has been demonstrated that epigenetic modifying agents can prime IFN γ -responsive loci and potentiate transcription following receptor binding [22, 23]. There was no change in the frequency of total tumor-infiltrating CD4+ T cells or regulatory T cells by flow cytometry; however, both CD4 and FoxP3 expression were significantly decreased at the mRNA level (Supplementary Table 1). Shen *et al.* demonstrated a similar decrease in FoxP3 mRNA transcripts following entinostat treatment in prostate cancer, suggesting that findings in both models may reflect reduced Treg suppressive function [24]. This idea will need to be confirmed in future studies.

Entinostat led to significant upregulation of the MHCII pathway at both the mRNA and protein levels. While NanoString[®] analysis showed no difference in mRNA expression of I-A or I-E alpha or beta chains with entinostat treatment, mRNA expression of the MHCII master regulator CIITA was significantly increased, and protein expression of MHCII was significantly upregulated as shown by flow cytometry. Although our prior *in vitro* data suggests that entinostat is able to upregulate MHCII expression on tumor cells directly [16], we did not observe a similar increase in MHCII expression in the immunocompromised Rag1 knockout mice. This suggests that induction of MHCII expression *in vivo* may be induced indirectly via IFN γ , which upregulates CIITA expression through the IFN γ -inducible pIV promoter [25], or other immune effectors, in combination with entinostat. While we did not evaluate the MHCI pathway at the protein level, mRNA expression of all

MHCI pathway genes investigated was significantly increased with entinostat treatment. Additionally, CIITA can contribute to MHCII expression via recruitment of the enhanceosome complex to site α and the SXY module [26]; hence, we would expect class II protein expression to also be upregulated in this model.

With entinostat treatment, PD-L1 expression was increased at the mRNA level and there was a trend towards increased expression at the protein level. This observation is in agreement with Abiko *et al.*, who noted that an increase in IFN γ expression in the tumor microenvironment can drive PDL1 expression on tumor cells. Specifically, they found that ovarian cancer tumor cells upregulate PD-L1 in response to IFN γ produced by cytotoxic T cells, leading to impaired effector functions [21], termed “adaptive resistance” [27, 28]. In their study, this increased PDL1 expression was associated with a poor prognosis, although PDL1 has also been associated with increased cytotoxic T cell infiltration and an improved prognosis in ovarian cancer patients [21, 29]. These inconsistent results demonstrate the respective contributions of pre-existing anti-tumor immune responses, as well as heterogeneity both within and between tumors in dictating outcome.

Interestingly, we found expression levels of canonical T cell immune checkpoint molecules LAG3 and BTLA to be decreased and PD-1 to be unchanged at the mRNA level in whole tumor lysates following entinostat treatment. Signaling through multiple immune checkpoint molecules drives T cell exhaustion, which permits tumor escape [30], and expression profiles of these proteins are regulated largely by epigenetic modifications [31, 32]. It is encouraging to speculate that entinostat may be able to alter the progression of T cell exhaustion in the tumor microenvironment for more durable anti-tumor immunity and better outcomes [33].

The immune effects of epigenetic agents were first studied in non-small cell lung cancer (NSCLC), when a group of patients who had been treated with the DNA methyltransferase inhibitor azacytidine subsequently received a checkpoint inhibitor; 60% of treated subjects achieved a durable clinical response [34]. In NSCLC cell lines, azacytidine was shown to induce expression of the MHCII pathway and PD-L1, as well as genes involved in several other important immune pathways [35]. In a diffuse B cell lymphoma cell line, treatment with entinostat led to significantly increased MHCII expression via CIITA [36], which is consistent with our findings of increased CIITA mRNA expression and increased MHCII protein expression. Importantly, tumor MHCII expression led to enhanced immune responses in preclinical studies of breast cancer, renal cell carcinoma, prostate cancer [37, 38], and, as we demonstrated herein, ovarian cancer. Furthermore, these findings have been supported in clinical studies of patients with breast and ovarian cancer. In both disease sites, increased tumor cell MHCII expression strongly correlates with higher numbers of infiltrating cytotoxic T cells, which in turn is associated with improved survival [18, 19, 39].

Several phase I and II clinical trials have investigated the use of HDAC inhibitors in ovarian cancer; however, the efficacy of these drugs appears limited when used as single agents or in combination with cytotoxic chemotherapy [40, 41]. Although our study was limited to one immunocompetent murine model and the sample sizes were small, our results suggest that treatment with entinostat leads to augmented adaptive effector functions and perhaps

reduced T cell exhaustion in ovarian cancer. Therefore, the most salient application of entinostat and other epigenetic modifiers, may be in combination with other immune-potentiating modalities, like checkpoint inhibitors, to stimulate more durable anti-tumor immunity in women with ovarian cancer. These findings warrant further investigation in more diverse immunocompetent murine ovarian cancer models as well as in patient-derived models.

Supplementary Material

Refer to Web version on PubMed Central for supplementary material.

Acknowledgments

Funding: This work was generously supported by the University of Alabama at Birmingham Center for Clinical and Translational Science Multidisciplinary Partner Network Pilot Program (grant UL1TR001417), the Foundation for Women's Cancer Ovarcome Grant, the Norma Livingston Foundation, the ABOG/AAOGF Scholarship Award, and the NIH T32 Research Training Program (CA091078).

References

1. Ozols RF, et al., Phase III trial of carboplatin and paclitaxel compared with cisplatin and paclitaxel in patients with optimally resected stage III ovarian cancer: a Gynecologic Oncology Group study. *J Clin Oncol*, 2003 21(17): p. 3194–200. [PubMed: 12860964]
2. Ledermann J, et al., Olaparib maintenance therapy in platinum-sensitive relapsed ovarian cancer. *N Engl J Med*, 2012 366(15): p. 1382–92. [PubMed: 22452356]
3. Pujade-Lauraine E, et al., Bevacizumab combined with chemotherapy for platinum-resistant recurrent ovarian cancer: The AURELIA open-label randomized phase III trial. *J Clin Oncol*, 2014 32(13): p. 1302–8. [PubMed: 24637997]
4. Aghajanian C, et al., Final overall survival and safety analysis of OCEANS, a phase 3 trial of chemotherapy with or without bevacizumab in patients with platinum-sensitive recurrent ovarian cancer. *Gynecol Oncol*, 2015 139(1): p. 10–6. [PubMed: 26271155]
5. Hamanishi J, et al., Safety and Antitumor Activity of Anti-PD-1 Antibody, Nivolumab, in Patients With Platinum-Resistant Ovarian Cancer. *J Clin Oncol*, 2015 33(34): p. 4015–22. [PubMed: 26351349]
6. Dawson MA and Kouzarides T, Cancer epigenetics: from mechanism to therapy. *Cell*, 2012 150(1): p. 12–27. [PubMed: 22770212]
7. Kim HJ and Bae SC, Histone deacetylase inhibitors: molecular mechanisms of action and clinical trials as anti-cancer drugs. *Am J Transl Res*, 2011 3(2): p. 166–79. [PubMed: 21416059]
8. Khabele D, et al., Drug-induced inactivation or gene silencing of class I histone deacetylases suppresses ovarian cancer cell growth: implications for therapy. *Cancer Biol Ther*, 2007 6(5): p. 795–801. [PubMed: 17387270]
9. Weichert W, et al., Expression of class I histone deacetylases indicates poor prognosis in endometrioid subtypes of ovarian and endometrial carcinomas. *Neoplasia*, 2008 10(9): p. 1021–7. [PubMed: 18714364]
10. Kim MG, et al., The relationship between cisplatin resistance and histone deacetylase isoform overexpression in epithelial ovarian cancer cell lines. *J Gynecol Oncol*, 2012 23(3): p. 182–9. [PubMed: 22808361]
11. West AC and Johnstone RW, New and emerging HDAC inhibitors for cancer treatment. *J Clin Invest*, 2014 124(1): p. 30–9. [PubMed: 24382387]
12. Skov S, et al., Cancer cells become susceptible to natural killer cell killing after exposure to histone deacetylase inhibitors due to glycogen synthase kinase-3-dependent expression of MHC class I-related chain A and B. *Cancer Res*, 2005 65(23): p. 11136–45. [PubMed: 16322264]

13. Khan AN, Gregorie CJ, and Tomasi TB, Histone deacetylase inhibitors induce TAP, LMP, Tapasin genes and MHC class I antigen presentation by melanoma cells. *Cancer Immunol Immunother*, 2008 57(5): p. 647–54. [PubMed: 18046553]
14. Woods DM, et al., The antimelanoma activity of the histone deacetylase inhibitor panobinostat (LBH589) is mediated by direct tumor cytotoxicity and increased tumor immunogenicity. *Melanoma Res*, 2013 23(5): p. 341–8. [PubMed: 23963286]
15. Maeda T, et al., Up-regulation of costimulatory/adhesion molecules by histone deacetylase inhibitors in acute myeloid leukemia cells. *Blood*, 2000 96(12): p. 3847–56. [PubMed: 11090069]
16. Turner TB, et al., Epigenetic modifiers upregulate MHC II and impede ovarian cancer tumor growth. *Oncotarget*, 2017.
17. Hamanishi J, et al., Programmed cell death 1 ligand 1 and tumor-infiltrating CD8+ T lymphocytes are prognostic factors of human ovarian cancer. *Proc Natl Acad Sci U S A*, 2007 104(9): p. 3360–5. [PubMed: 17360651]
18. Forero A, et al., Expression of the MHC Class II Pathway in Triple-Negative Breast Cancer Tumor Cells Is Associated with a Good Prognosis and Infiltrating Lymphocytes. *Cancer Immunol Res*, 2016 4(5): p. 390–9. [PubMed: 26980599]
19. Callahan MJ, et al., Increased HLA-DMB expression in the tumor epithelium is associated with increased CTL infiltration and improved prognosis in advanced-stage serous ovarian cancer. *Clin Cancer Res*, 2008 14(23): p. 7667–73. [PubMed: 19047092]
20. Peart MJ, et al., Identification and functional significance of genes regulated by structurally different histone deacetylase inhibitors. *Proc Natl Acad Sci U S A*, 2005 102(10): p. 3697–702. [PubMed: 15738394]
21. Abiko K, et al., PD-L1 on tumor cells is induced in ascites and promotes peritoneal dissemination of ovarian cancer through CTL dysfunction. *Clin Cancer Res*, 2013 19(6): p. 1363–74. [PubMed: 23340297]
22. West AC, et al., An intact immune system is required for the anticancer activities of histone deacetylase inhibitors. *Cancer Res*, 2013 73(24): p. 7265–76. [PubMed: 24158093]
23. Sumpf K, et al., Histone deacetylase inhibitor MS-275 augments expression of a subset of IFN-gamma-regulated genes in *Toxoplasma gondii*-infected macrophages but does not improve parasite control. *Exp Parasitol*, 2017.
24. Shen L, et al., Class I histone deacetylase inhibitor entinostat suppresses regulatory T cells and enhances immunotherapies in renal and prostate cancer models. *PLoS One*, 2012 7(1): p. e30815. [PubMed: 22303460]
25. Muhlethaler-Mottet A, et al., Expression of MHC class II molecules in different cellular and functional compartments is controlled by differential usage of multiple promoters of the transactivator CIITA. *EMBO J*, 1997 16(10): p. 2851–60. [PubMed: 9184229]
26. Gobin SJ, et al., Site alpha is crucial for two routes of IFN gamma-induced MHC class I transactivation: the ISRE-mediated route and a novel pathway involving CIITA. *Immunity*, 1997 6(5): p. 601–11. [PubMed: 9175838]
27. Taube JM, et al., Colocalization of inflammatory response with B7-h1 expression in human melanocytic lesions supports an adaptive resistance mechanism of immune escape. *Sci Transl Med*, 2012 4(127): p. 127ra37.
28. Spranger S, et al., Up-regulation of PD-L1, IDO, and T(regs) in the melanoma tumor microenvironment is driven by CD8(+) T cells. *Sci Transl Med*, 2013 5(200): p. 200ra116.
29. Webb JR, et al., PD-L1 expression is associated with tumor-infiltrating T cells and favorable prognosis in high-grade serous ovarian cancer. *Gynecol Oncol*, 2016 141(2): p. 293–302. [PubMed: 26972336]
30. Wherry EJ and Kurachi M, Molecular and cellular insights into T cell exhaustion. *Nat Rev Immunol*, 2015 15(8): p. 486–99. [PubMed: 26205583]
31. Pauken KE, et al., Epigenetic stability of exhausted T cells limits durability of reinvigoration by PD-1 blockade. *Science*, 2016 354(6316): p. 1160–1165. [PubMed: 27789795]
32. Sen DR, et al., The epigenetic landscape of T cell exhaustion. *Science*, 2016 354(6316): p. 1165–1169. [PubMed: 27789799]

33. Zhang F, et al., Epigenetic manipulation restores functions of defective CD8(+) T cells from chronic viral infection. *Mol Ther*, 2014 22(9): p. 1698–706. [PubMed: 24861055]
34. Chiappinelli KB, et al., Combining Epigenetic and Immunotherapy to Combat Cancer. *Cancer Res*, 2016 76(7): p. 1683–9. [PubMed: 26988985]
35. Wrangle J, et al., Alterations of immune response of Non-Small Cell Lung Cancer with Azacytidine. *Oncotarget*, 2013 4(11): p. 2067–79. [PubMed: 24162015]
36. Cycon KA, et al., Histone deacetylase inhibitors activate CIITA and MHC class II antigen expression in diffuse large B-cell lymphoma. *Immunology*, 2013 140(2): p. 259–72. [PubMed: 23789844]
37. Mortara L, et al., CIITA-induced MHC class II expression in mammary adenocarcinoma leads to a Th1 polarization of the tumor microenvironment, tumor rejection, and specific antitumor memory. *Clin Cancer Res*, 2006 12(11 Pt 1): p. 3435–43. [PubMed: 16740768]
38. Hillman GG, et al., Turning tumor cells in situ into T-helper cell-stimulating, MHC class II tumor epitope-presenters: immuno-curing and immuno-consolidation. *Cancer Treat Rev*, 2004 30(3): p. 281–90. [PubMed: 15059651]
39. Leffers N, et al., Identification of genes and pathways associated with cytotoxic T lymphocyte infiltration of serous ovarian cancer. *Br J Cancer*, 2010 103(5): p. 685–92. [PubMed: 20664601]
40. Modesitt SC, et al., A phase II study of vorinostat in the treatment of persistent or recurrent epithelial ovarian or primary peritoneal carcinoma: a Gynecologic Oncology Group study. *Gynecol Oncol*, 2008 109(2): p. 182–6. [PubMed: 18295319]
41. Dizon DS, et al., A phase II evaluation of belinostat and carboplatin in the treatment of recurrent or persistent platinum-resistant ovarian, fallopian tube, or primary peritoneal carcinoma: a Gynecologic Oncology Group study. *Gynecol Oncol*, 2012 125(2): p. 367–71. [PubMed: 22366594]

Author Manuscript

Author Manuscript

Author Manuscript

Author Manuscript

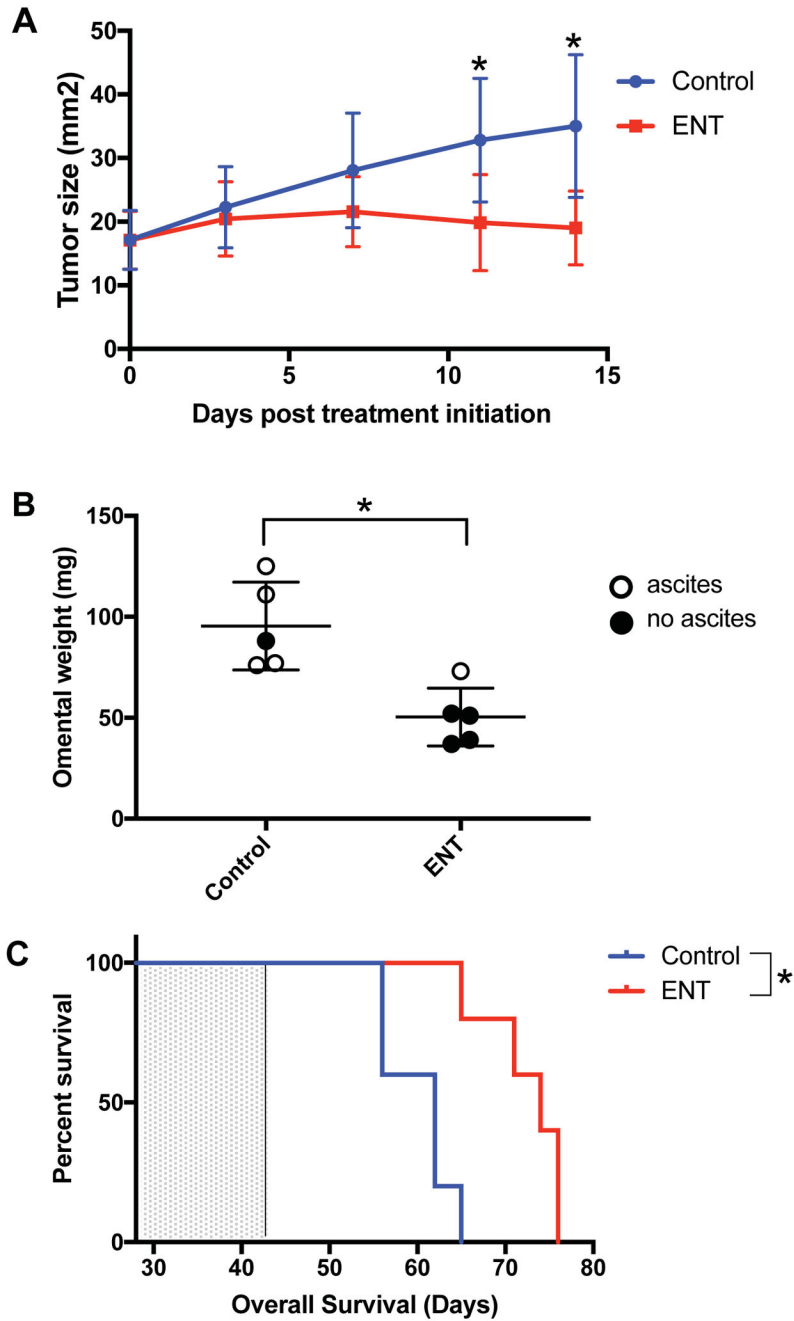


Figure 1: Entinostat (ENT) inhibits tumor growth and prolongs survival in a syngeneic murine ovarian cancer model.

A) ENT treatment led to a significant decrease in tumor growth compared to vehicle in a subcutaneous ID8 model by day 11 of treatment (19.9 vs. 32.9 mm², p=0.046), which persisted at day 14 (19.0 vs. 35 mm², p=0.022). Treatment was started at 32 days post tumor implantation. Data shown is representative of 3 experiments. Error bars represent standard deviation. B) In an intraperitoneal ID8 model, ENT treatment led to a significant decrease in omental tumor weight compared to vehicle (44.7 vs. 100.4 mg, p<0.001), and fewer ENT-treated mice had ascites at time of tumor harvesting. Data shown is representative of 2

experiments. C) ENT treatment significantly prolonged overall survival (OS) compared to vehicle in an intraperitoneal ID8 model (median OS 74 vs 62 days, $p=0.005$, HR 0.26 (95% CI 0.06–1.21)). Mice were treated from day 28 to 42 (indicated by shaded portion of graph). $n=5$ mice per group. *indicates $p<0.05$

Author Manuscript

Author Manuscript

Author Manuscript

Author Manuscript

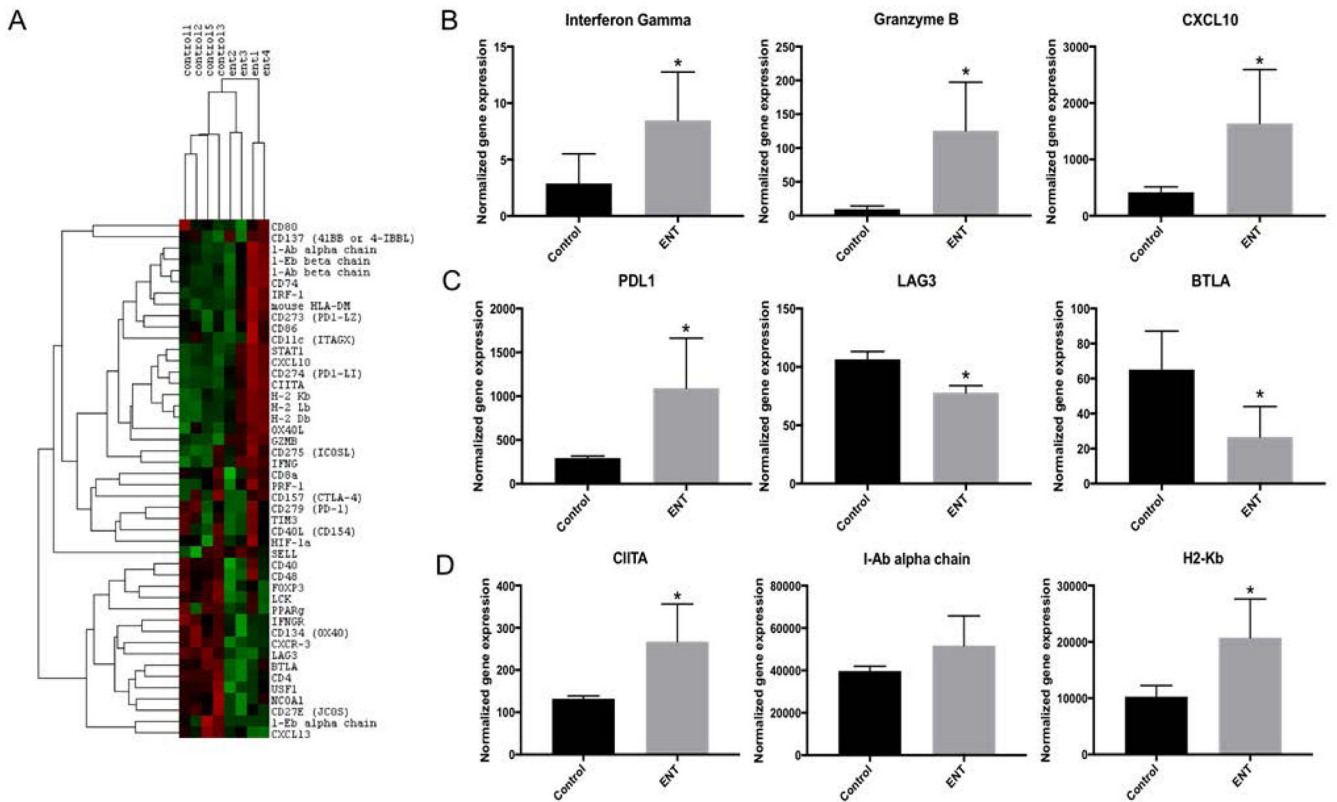


Figure 2: By NanoString[®] analysis, entinostat (ENT) induces significant changes in mRNA expression of multiple genes involved in anti-tumor immunity.

C57Bl/6 mice were treated with either ENT or vehicle control for 14 days (n=4 per group). NanoString[®] analysis was performed on omental tumors. A) In a selected panel of 50 genes specific to the adaptive immune response, unsupervised hierarchical clustering shows distinct gene expression patterns in omental tumors from C57Bl/6 mice treated with ENT compared to vehicle controls. Green indicates downregulated genes, while red indicates upregulated genes. B) ENT treatment led to a significant increase in expression of T cell effector molecules, including interferon gamma (8.5 vs. 2.9, p=0.039), granzyme B (125.4 vs. 9.5, p=0.008), and CXCL10 (1,636.4 vs. 417.0, p=0.023). C) ENT-treated mice showed significantly increased expression of the immune checkpoint molecule PDL1 (1,090.6 vs. 294.2, p=0.016) and significant decreases in immune checkpoints LAG3 (78.0 vs. 106.5, p<0.001) and BTLA (26.6 vs. 65.11, p=0.017). D) ENT treatment significantly increased expression of CIITA (267.4 vs. 132.1, p=0.011) and the MHCI pathway (20,728.3 vs. 10,272.8, p=0.013). There was a trend towards increased MHCII pathway expression, although this was not statistically significant (51,667.3 vs. 39,683.12, p=0.098). H2-Kb and I-Ab alpha chain are shown and are representative of the other genes in the MHCI and MHCII pathways, respectively. *indicates p<0.05

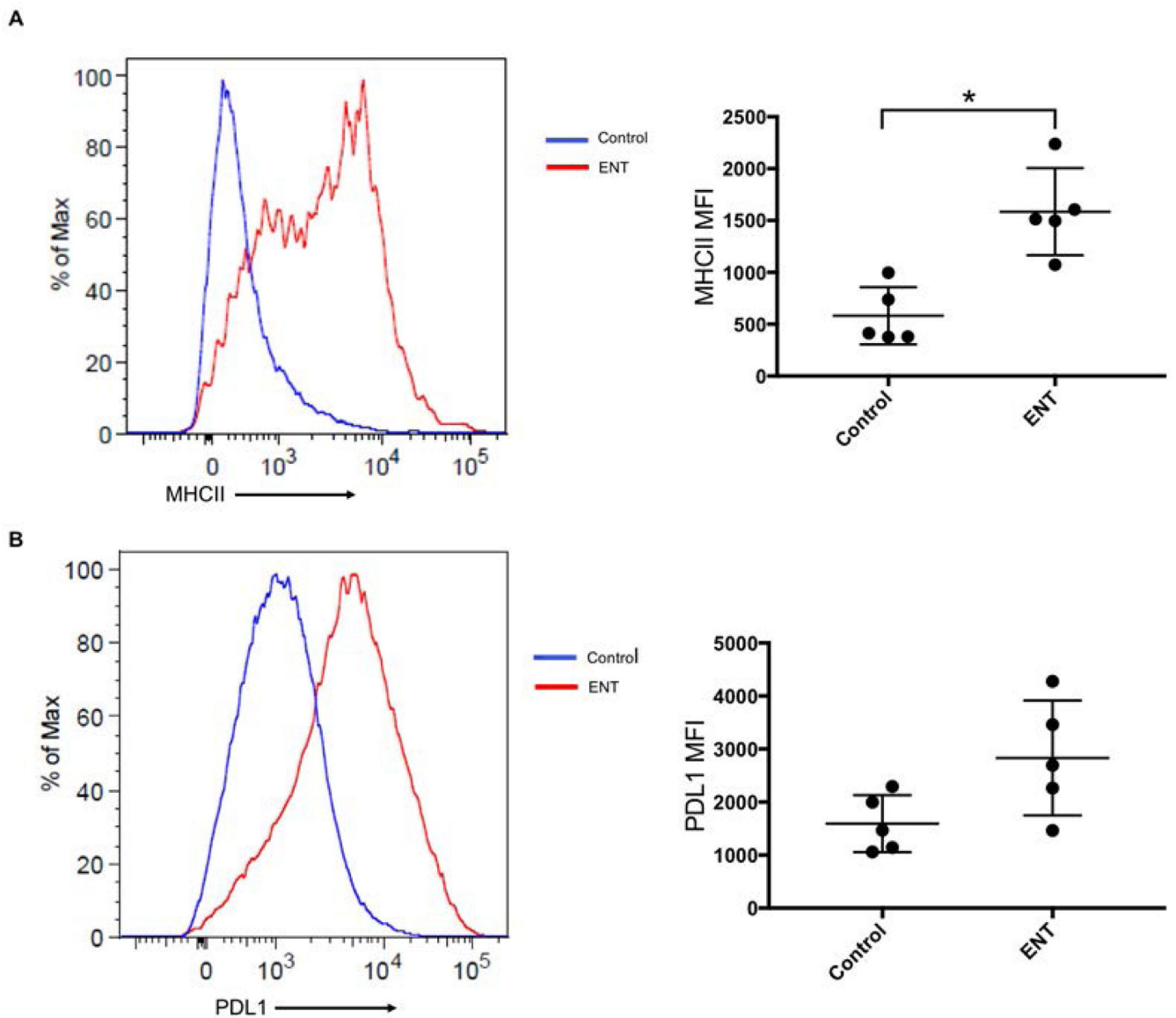


Figure 3: Entinostat (ENT) increases MHCII and PDL1 expression on omental tumor cells. Gating was on single, viable, CD45 negative cells. Expression was compared using mean fluorescent intensity (MFI). A) ENT treatment led to significant increase in MHCII expression (1,585.0 vs. 581.4 MFI $p=0.002$). B) ENT treatment led to a near-significant increase in PDL1 expression (2,832.0 vs. 1,593.0, $p=0.052$). $n=5$ mice per group. *indicates $p<0.05$.

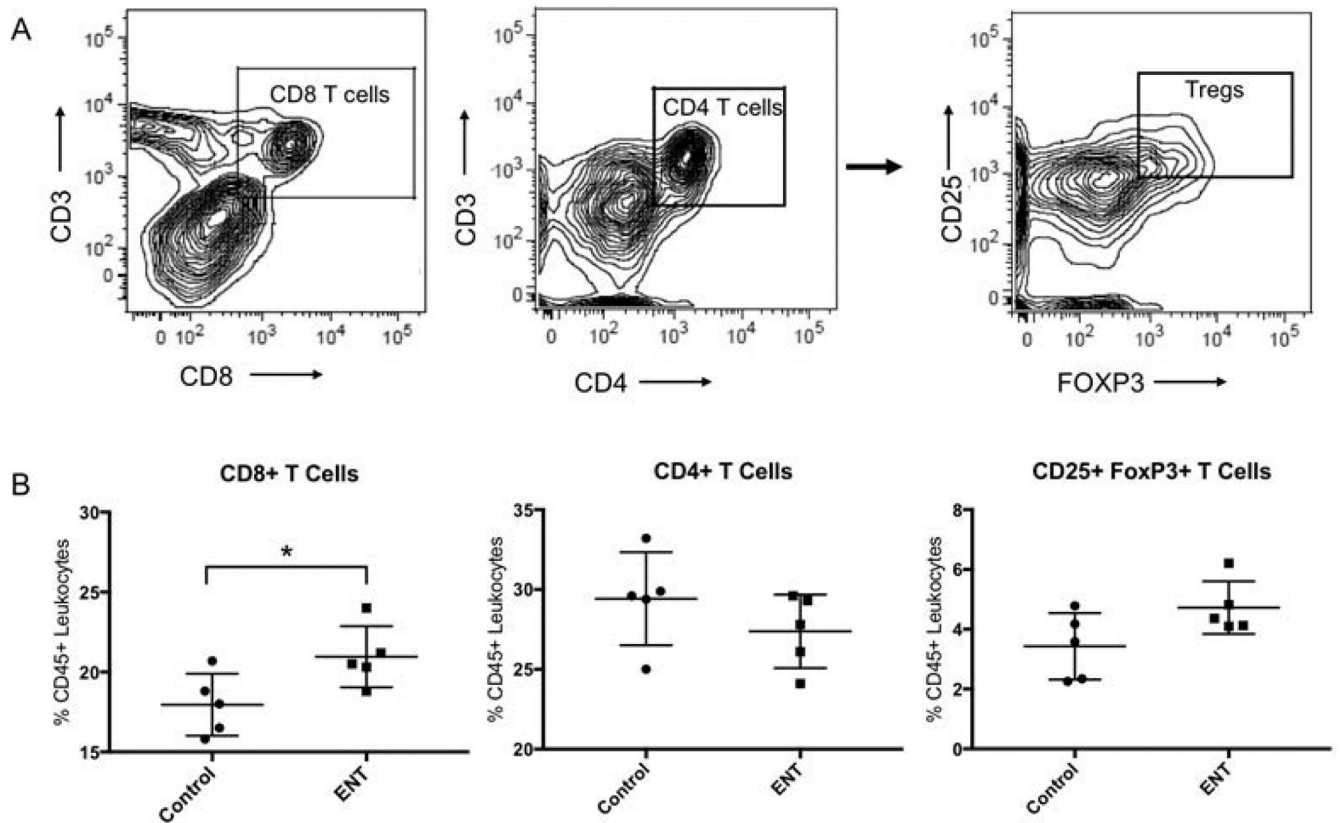


Figure 4: Entinostat (ENT) increases recruitment of CD8+ T cells into the tumor.

A) Gating strategy for identification of CD8+ and CD4+ T cells and CD25+FoxP3+ T cells (Tregs). Initial gating was on single, viable, CD45+ cells. B) Entinostat treatment increased the percentage of CD8+ T cells in omental tumors of C57bl/6 mice (21.0% vs. 18.0%, $p=0.039$). There was no difference in percentage of CD4 T cells (27.4% vs. 29.4%, $p=0.255$) or Tregs (4.7% vs. 3.4%, $p=0.075$). $n=5$ mice per group. *indicates $p<0.05$.

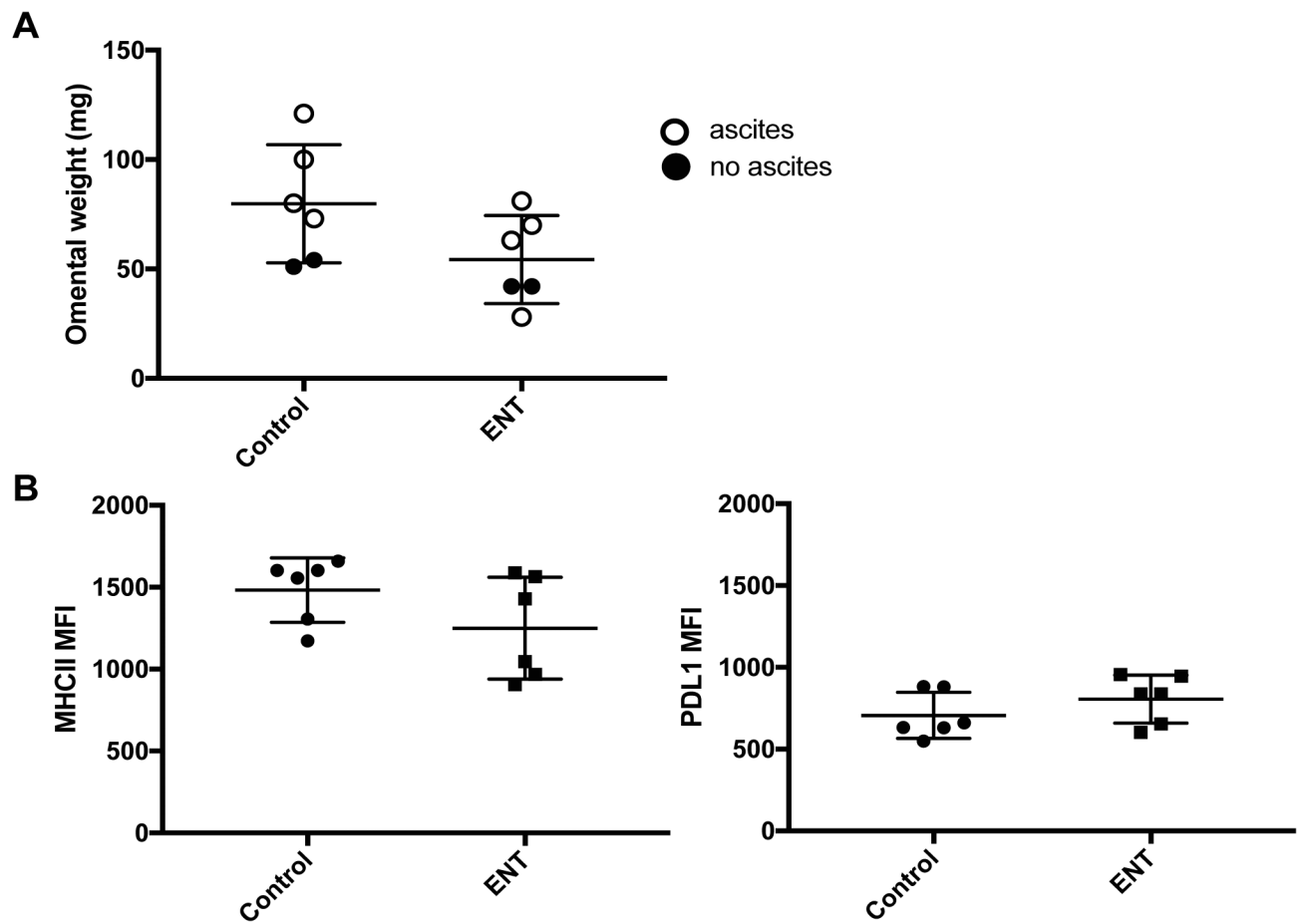


Figure 5: Entinostat (ENT) does not significantly inhibit tumor growth or increase MHCII or PDL1 expression in Rag1 knockout mice.

A) In Rag1 knockout mice, there was no difference in omental tumor weight between mice treated with ENT versus vehicle control (54.3 vs. 79.8 mg, $p=0.093$) and no difference in ascites formation. B) There was no difference in either MHCII (1,250.0 vs. 1,483.0 MFI, $p=0.152$) or PDL1 expression (805.8 vs. 706.0 MFI, $p=0.258$) in Rag1 knockout mice treated with ENT versus vehicle control. $n=6$ mice per group.